Improving the Performance of Nuclear Quadrupole Resonance Sensing Technologies for in situ Detection of Narcotics and Explosives

Dan. J. Parrish[1], Mona Ibrahim[1,*], Tim W.C. Brown[2], Richard. I. Jenkinson[3] and Peter J. McDonald[1]

[1] Department of Physics, University of Surrey, Guildford, GU2 7XH, UK

[2] Institute for Communication Systems, University of Surrey, Guildford, GU2 7XH, UK

[3] Defence Science and Technology Laboratory, Fort Halstead, Sevenoaks, TN14 7BP, UK

* Correspondence: d.parrish@surrey.ac.uk, Tel.: +44-7462-060-603

Abstract

Nuclear Quadrupole Resonance (NQR) and Nuclear Magnetic Resonance (NMR) are spectroscopic techniques that offer the ability to characterise samples non-destructively *in situ* for quality control in industrial processes (e.g., water content in food), and for detection of explosives and narcotics in defence and security sensing applications. Current NMR-/ NQR-based sensing technologies can achieve good performance in a controlled laboratory environment where the effect of external Radio Frequency Interference (RFI) can be mitigated by RFI shielding. However, for *in situ* sensing applications outside the laboratory, complete physical shielding is often not possible or not practical (heavy, bulky) and therefore alternative methods are needed for NMR-/ NQR-based sensing technologies to be useful.

This EngD project focusses on the development of methods for active elimination of RFI for *in situ* sensing applications of NMR and NQR. The work aims to develop signal processing techniques that work with varying degrees of physical suppression (RFI shielding), to improve the accuracy and reliability of the NMR-/ NQR-based sensing technologies. The approach being developed is a machine learning process in which RFI is automatically identified using a decision tree model followed by an RFI suppression algorithm to produce the RFI-minimised signal.

This talk describes the development of an experimental testbed for data collection and some recent results achieved by applying the algorithms to measured NQR data subject to simulated burst mode RFI. The performance of the decision tree model is validated against human operator performance data, generated by volunteers rating the degree to which they can confidently declare an NQR signal present or not in RFI-polluted data. The performance of the model is quantified as a Receiver Operating Characteristic (ROC) curve, which plots true positive against false positive for a binary classifier. For the data described here, the decision tree model improved (relative to no RFI removed) the area under curve (AUC) value from 0.58 to 0.906, where AUC = 1 means a 100% detection rate with a 0% false alarm rate.

1 - Introduction

Nuclear Magnetic Resonance (NMR) and Nuclear Quadrupole Resonance (NQR) are spectroscopic techniques typically used to characterise materials and processes in a laboratory environment. There is a growing demand for *in situ* sensing applications, with some being already established, such as oil-well logging (1) and food processing (2). There are also opportunities where NMR and NQR could be used for quality control and assurance in civil engineering applications (3), as well as for security screening (4).

However, making NMR and NQR work in these field applications presents many difficulties because of the low operating frequencies (e.g., 1 – 10MHz). In NMR, for a given nucleus (e.g., hydrogen) the frequency is defined by the strength of the external magnetic field. In NQR, where there is no

external magnetic field, for a given quadrupolar nucleus (e.g., nitrogen) the frequency is defined by an internal electric field gradient. In both cases, low frequency means a low signal-to-noise ratio (SNR) and spectra that can be dominated by noise. Therefore, noise suppression methods are needed.

The noise can be separated into two types: incoherent noise such as the thermal white noise from the NQR/NMR sensor, and coherent noise. The coherent noise can itself be divided into two: internal acoustic ringing from the tuned coil after each RF excitation pulse and detected externally broadcast Radio Frequency Interference (RFI), such as power supplies or aircraft communications.

Noise suppression techniques do exist to improve the SNR, for example, acoustic ringing can be reduced by appropriate phase cycling in the excitation pulse sequence (5). Thermal noise in the tuned coil can be reduced by repeating the experiment and averaging the NMR/NQR signal. However, the nature of RFI means that signal averaging and phase cycling are not effective. The RFI can also vary greatly from one location to another making suppression challenging. Other suppression techniques, such as using a bandpass filter are not effective because there is a wide range of RFI carrier frequencies that can be encountered. Faraday shielding, which attenuates external RFI, can increase SNR but is not necessarily suitable for *in situ* applications.

Techniques have been developed for suppression of coherent RFI. Garroway *et al*. (6) developed methodology using additional RF coils, identical to the NQR coil, which were placed near to the NQR coil and recorded just the background RFI occurring at the same time as the NQR measurement. The additional receiver coil data was then used to produce an estimate of the background RFI at the NQR site measurement. This was subtracted from the contaminated NQR signal to reveal the true NQR signal. A detection rate of 100%, with 0.25% false alarm rate was achieved in detection trials with buried landmines. Despite the performance achieved in trials, other technological limitations, as well as wider system considerations, meant the NQR sensor was not developed beyond a prototype.

Tantum *et al*. (7) developed signal processing based on a least mean squares technique for a single NMR/NQR sensor. The authors used this to produce an estimate of the background RFI, and then apply a Bayesian discriminant algorithm which extracted the NQR signal from the data. This technique produced a detection rate of 85% with a false alarm rate of 15%.

Shao *et al.* (8) developed an advanced signal filtering technique called ‘interference-cancelled echo-train approximation’ designed to target RFI that has a significant fraction of spectral width very close to, but not on, the NQR frequency. The technique achieved a detection rate of 95% with a false alarm rate of 5%, but the authors used simulated RFI that did not have the spectral complexity of measured RFI. The same authors (9) followed up with a modified version of their original technique that could cope with more complex RFI, including non-stationary RFI, and achieved a 90% detection rate, with 10% false alarm rate.

An increasing proportion of external RFI is digital in nature and occurs in short bursts. This is especially true in RF saturated environments, such as airports. Therefore, this project is working on a new and novel approach to use machine learning to treat ‘burst mode’ digital RFI. It aims to remove the need for Faraday shielding and attempts to increase the SNR of NMR/NQR experiments to improve their detection rate/usability for *in-situ* applications.

To address this problem, work was undertaken to characterise real-world background RFI in order to better understand how to suppress it. An experimental testbed was created to acquire NQR data as well as the ability to control the RFI injected into the NQR data. The testbed data was processed using a machine learning based RFI identification method and simple suppression method to

produce RFI suppressed data, which was then used in a validation trial using volunteer raters. The results from the validation process produced the Area Under the Curve (AUC) value for the ROC curves for this RFI suppression method, allowing it to be compared with other RFI suppression methods.

2 – Methodology

2.1 – RFI Characterisation

Due to the increase in the adoption of digital technology, a larger proportion of RFI is digital, which is usually 'burst mode'. This means RF signal arrives in groups of pulses, typically mV in amplitude, which easily masks the substantially smaller NMR/NQR signal, which are typically μV in amplitude.

To better understand the RFI, it was characterised to extract key parameters in the following manner:

1 – The recorded RFI is plotted in the time domain, showing the RFI pulses in the raw RF signals.

2 – The RFI is Fourier transformed to obtain the frequency spectrum of the data, to see how it overlaps with frequencies used by NMR/NQR equipment and how it varies for different locations.

3 – The RFI is filtered and thresholded using a moving average top hat filter, which made the pulses stand out more clearly from the rest of the recording, making them easier to threshold. This thresholded data created a binary mask of where the RFI was in each RFI recording.

4 – The binary data is used to calculate multiple different parameters about the RFI, including;

- Average RFI pulse length
- Average time gap between RFI pulses
- Percentage of RFI recording that has digital RFI present

5 – The binary data is put through an autocorrelation function to find repeating patterns within the RFI data, which reveal the coherent nature of digital RFI. Peaks in the results plotted as a function of time indicate repetition times within the original dataset.

6 – The RFI at specific frequencies within the RFI recording can be focused on by applying a Gaussian filter at the chosen frequency to the Fourier transformed data [frequency domain], zeroing out the rest of the Fourier transformed data. This filtered data is then inverse Fourier transformed to produce the [time domain] data of the RFI at the specific frequency only. This allows comparisons to be made between continuous RF RFI and burst mode RFI which all occur at different frequencies within the same overall RFI recording.

7 – The time-domain data is put through the same autocorrelation function to find repeating patterns within the data. This allows the repeating patterns at different frequencies to be compared to show the different RFI within the same recording.

2.2 – Experimental Testbed

The testbed comprised the NQR coil and RFI coils in a wooden box covered with EM shielding cloth to make the Faraday enclosure. This ensured only the pseudo-RFI was present in the NQR data.

Sodium nitrite ($NaNO_2$) was used as a sample for development of the method as it has ^{14}N NQR frequencies (1, 3.6 and 4.6 MHz) that fit within the range of those found in narcotic and explosive materials. The chosen frequency for this testbed was 3.6 MHz.

This project used the 'CPMG' NQR pulse sequence [10], illustrated in Figure 1. This sequence uses excitation pulses to create 'echo' signals, which decrease in amplitude with each subsequent excitation pulse. The echo intensities can be fit to an exponential decay to produce the T_2 value of the sample, where T_2 is a characteristic NMR/ NQR time constant of a material. Experiments were repeated 64 times with random pseudo-RFI injected for each repetition. Each repetition is known as a 'scan'.

Pseudo-RFI was generated using a binary mask of RFI recordings measured at the University of Surrey, which contained real-world pulsed RFI. The source of this RFI is likely to be linked to the local Gatwick and Heathrow airports. The carrier and sideband frequencies of the pseudo-RFI were Gaussian distributed around the NQR frequency, whilst the amplitude and phase were linearly distributed.

The main NQR coil contains the sample, transmits the radio-frequency NQR excitation pulses and detects the NQR signals as well as RFI. The sample coil was 14 cm long and 7.8 cm in diameter and tuned to 3.6 MHz with a bandwidth of 0.07 MHz. The NQR coil is mounted centrally within the enclosure with additional identical coils mounted orthogonally to the NQR coil. These additional coils act as receiver coils and record the background RFI that occurs at the same time as the NQR experiment. These provide additional recorded data that can be used in future work for different RFI suppression techniques.

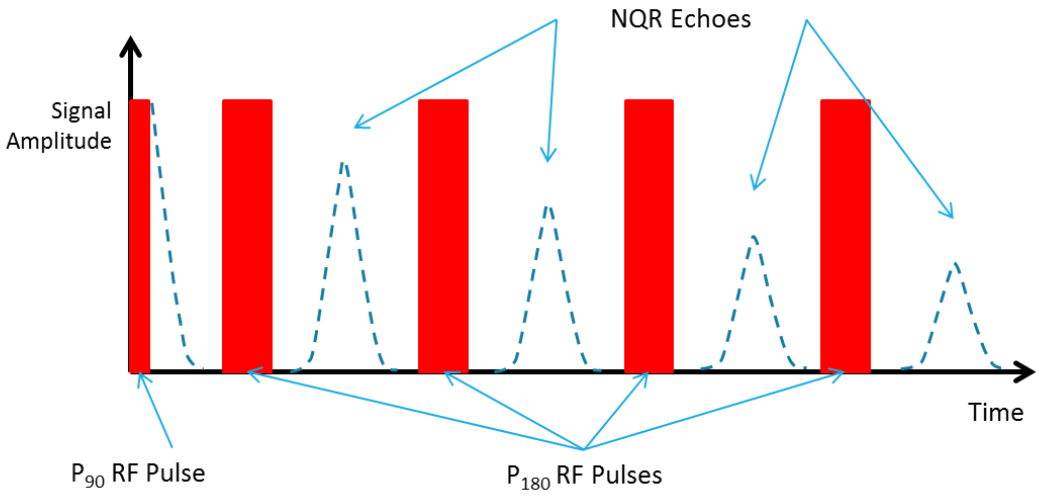

Figure 1 - Illustration of a CPMG pulse experiment, showing the RF pulses (RED) and the NMR/NQR signal (Blue)

The three RFI transmission coils have a height of 5 mm and a diameter of 15 cm. These were mounted orthogonal to the NQR coil on the inside of the shielded enclosure equidistant from the central NQR coil. The RFI was transmitted using two arbitrary waveform generators (PXIe, National Instruments).

The NQR excitation pulses were created using a Tecmag Redstone spectrometer, amplified and then transmitted by the NQR coil. The resulting NQR signals were detected and processed by the Redstone in the traditional way in parallel to all of the raw signals being recorded by an oscilloscope

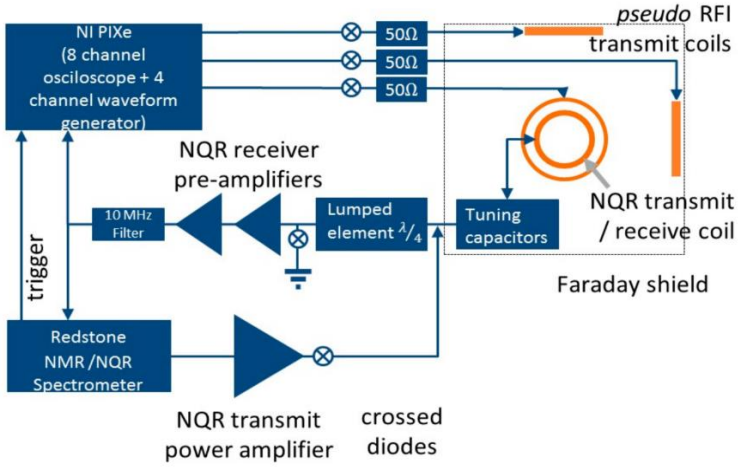

Figure 2 - Schematic diagram of the experimental testbed (10)

card, using an oversampled rate of 10.8 MHz. The cards were all run by a single computer running in a National Instruments PXIe chassis. The schematic of the entire testbed system is illustrated in Figure 2.

2.3 – Decision Tree Model

Development of the machine learning process described here was undertaken as part of a larger project (10) and recently reported by Ibrahim *et al*. (11). Various different machine learning models were tested to determine their RFI detection rate for the same training dataset. The results yielded detection efficiencies as follows: K-nearest neighbours (KNN) = 95 %; Support Vector Machine (SVN) = 91 %; Decision Tree (DT) = 98.2 %. On the basis of the detection rates the decision tree model was adopted.

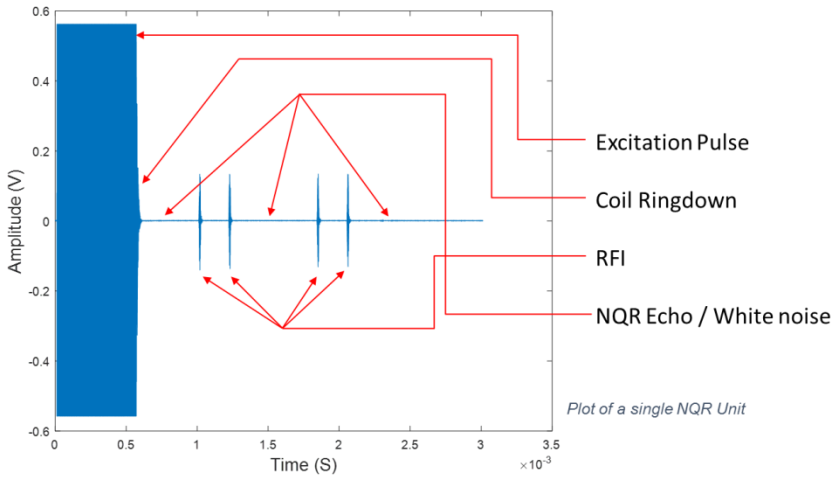

Figure 3 - Illustration of a single unit of data with different components labelled

Processing the NQR data starts by breaking down each sequence of NQR echoes into individual records, which we label as units, illustrated in Figure 3. These units consist of data classes that are the excitation pulse, the ringdown from the coil following the pulse, any RFI that may be present, and remaining data that is 'echo'. White noise is also included in the 'echo' class because the model is only looking to identify RFI that will need to be removed. The decision tree model is trained to classify windows of data into one of these four classes: 'pulse', 'ringdown', 'RFI' or 'echo'. To

determine the correct class to assign, it uses the values of 27 features which are calculated for each window of data. These features include the 75th percentile value of the window of data, the maximum frequency, the average of the derivative of the data, the starting time of the window of data and the sum of all of the peaks in the data. The window of data comes from a sliding window that passes through each unit of data to be processed. Each window is assigned a class value by the model, which is used to create a binary mask of all data points which were classified as 'RFI'.

The decision tree (DT) model was trained using labelled data recorded with pseudo-RFI. The binary masks used to produce the pseudo-RFI were used to label the RFI in the data. Additional binary masks were produced that represent where the pulse, ringdown and echo are expected. These are produced from the timing parameters of the experiment and are used to label the relevant parts of the data. The model used for validation and processing had been trained on over 50,000 units of data, where a normal 64 scan experiment will produce 512 units.

Once all data points have been classified, the data is demodulated using the MATLAB demodulation function, with a 10kHz low pass filter applied. At this stage, the data is equivalent to that acquired by the spectrometer.

We suppressed the RFI using a method we termed 'direct removal', illustrated in Figure 4. This method replaces the identified RFI with the weighted average of data from the same time window from other units that had no RFI at that given time.

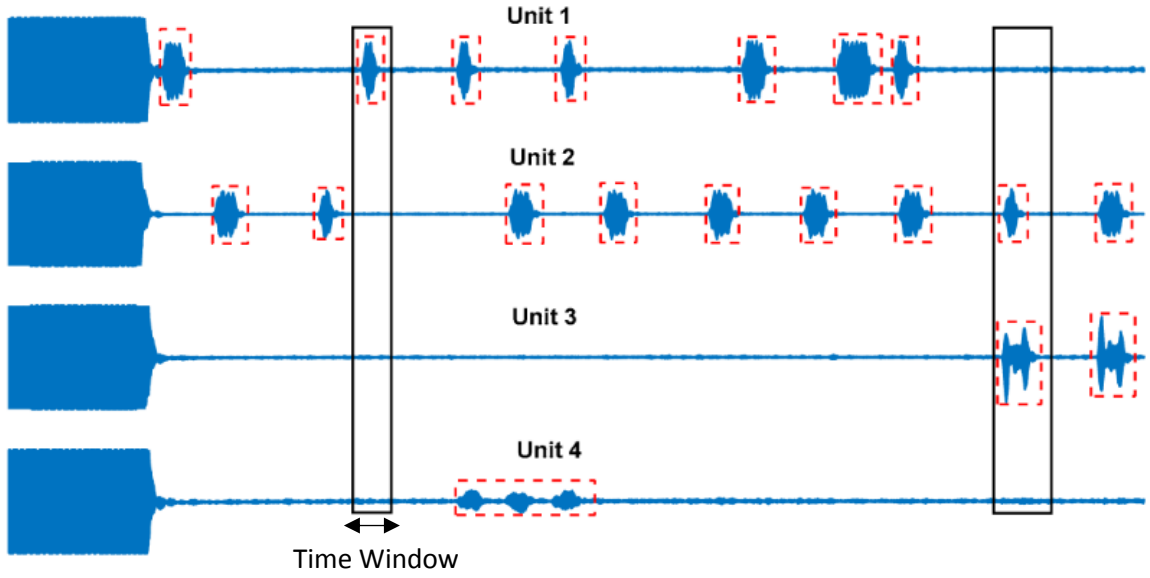

Figure 4 - Illustration of the direct removal RFI suppression method [10]

The final step is to average the units across all scans of the experiment, accounting for the phase cycling through the scans, to produce a final average of the NMR/NQR signal, with the RFI suppressed. Figure 5 shows the full process in flowchart form.

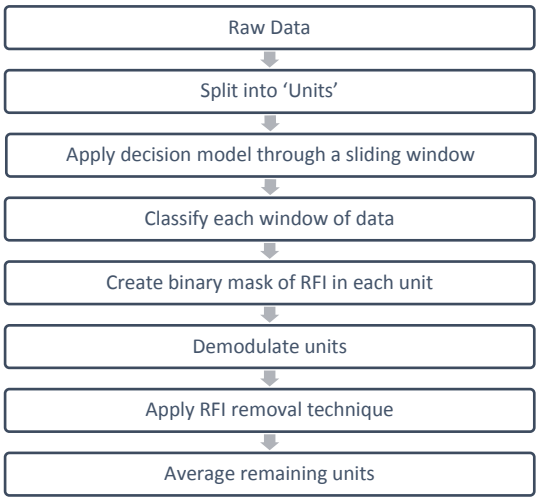

Figure 5 - Flowchart of the RFI identification and suppression process

2.4 – Validation of the Decision Tree RFI identification and RFI Direct Removal

A validation trial using volunteer raters was undertaken to determine the effectiveness of the RFI suppression method. The number of scans was varied to quantify the performance (e.g., Area Under the ROC Curve value per scan) to allow comparison with other RFI suppression techniques. Volunteers were shown 'good' NQR data and 'bad' non-processed RFI data. They were shown 100 datasets, of which 90 were random datasets from the entire available collection, and the final 10 were repeat showings of random datasets from the original 90. The repeating datasets were to see if the ratings provided by the same volunteer changed between viewings. The datasets shown were either Processed or Non-Processed by the RFI suppression technique. Specific comparisons were made between:

- Data identification when data only included Pseudo RFI contamination and when it also included No-Pseudo RFI in order to check that the method did not make things worse.
- Varying Sample Weight (0, 50, 100, 150 or 200g $NaNO_2$) to investigate sensitivity.
- Final averaged signal produced from either 4, 8, 16, 32 or 64 scans in order to find the minimum scans required for adequate detection rate.

The volunteers had to rate each dataset they were shown, from '0' to '10', where '0' means no NQR signal definitely seen; '10' means NQR signal definitely seen and '5' means could not decide.

Results from the validation trial were plotted as Receiver Operating Characteristic (ROC) curves. This plots true positive declarations against false positive declarations as a method of quantifying the detection performance of a binary sensor. To compare different ROC curves, the Area Under the Curve (AUC) is calculated, where a value of 1 is 100% detection rate with 0% false alarm whilst a value of 0.5 is the equivalent of guessing, such as flipping a coin.

3 – Results

3.1 – RFI Characterisation

To show the variety of RFI present in the environment, RFI was recorded at several locations, including:

- NMR Lab at the University of Surrey;
- NQR Lab at Dstl;
- Another indoor location at the University of Surrey away from the NMR laboratory;
- Outdoor location at the University of Surrey.

Figure 6 shows 500 µs of time-domain data for RFI recorded at the locations listed above. Each record reveals the presence of digital pulses, of varying character, at each location. Figure 7 shows the spectra (Fourier Transform) of the time domain data shown in Figure 6, with the spectrum of the Dstl lab being two orders of magnitude smaller in amplitude. Figure 8 shows the result of the autocorrelation function when applied to the binary mask of the data in Figure 6.

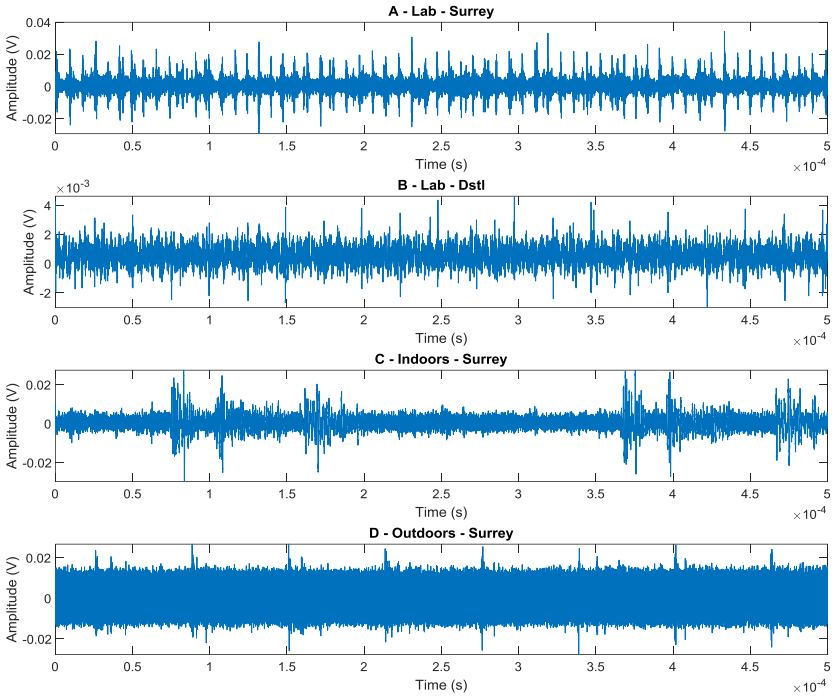

Figure 6 - Plot showing 500 us of raw RFI measured at: A = NMR lab at Surrey, B = NQR lab at Dstl, C = Indoor Location at Surrey, D = Outdoor Location at Surrey

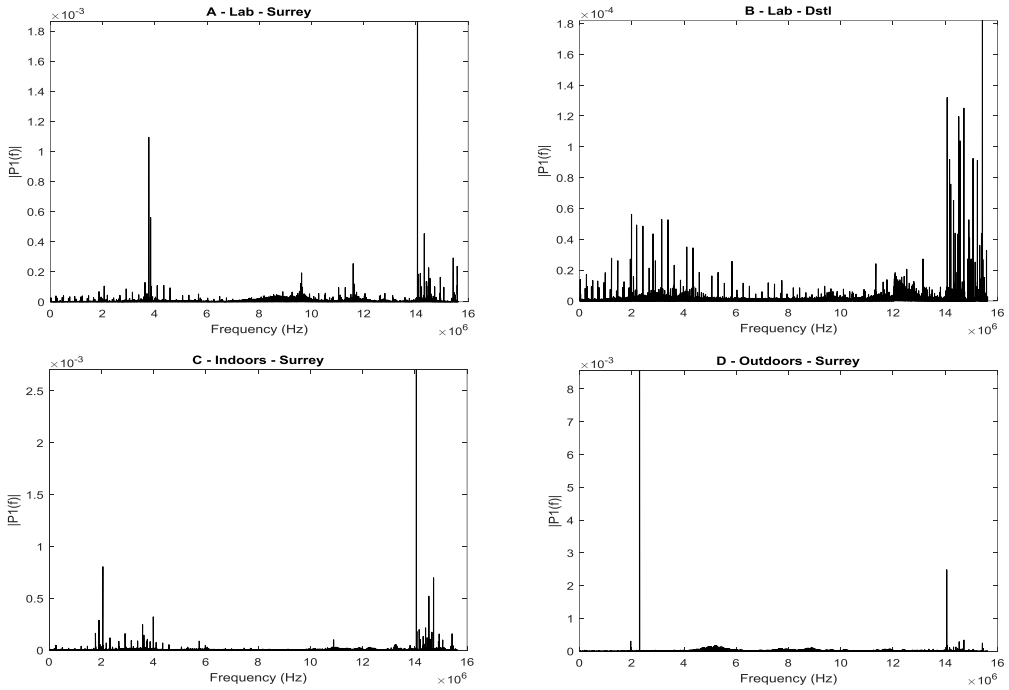

Figure 7 - Fourier Transform Plots of RFI measured at: A = NMR lab at Surrey, B = NQR lab at Dstl, C = Indoor Location at Surrey, D = Outdoors Location at Surrey

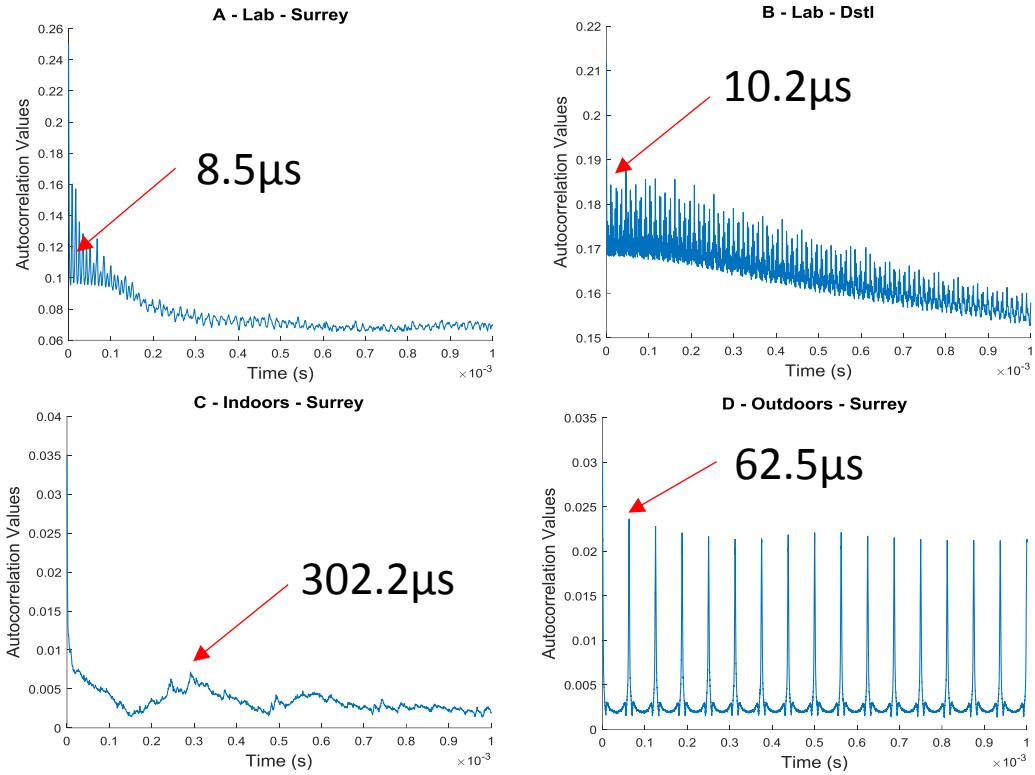

Figure 8 - Autocorrelation Results, with highlighted repetition times, for RFI measured at: A = NMR lab at Surrey, B = NQR lab at Dstl, C = Indoor location at Surrey, D = Outdoors location at Surrey

Figure 9 shows that the autocorrelation for the Indoor recording (Fig. 8c) has minor autocorrelation up to the 1 ms. However, when the whole data length is plotted, a repetition time of 10 ms becomes clearly visible.

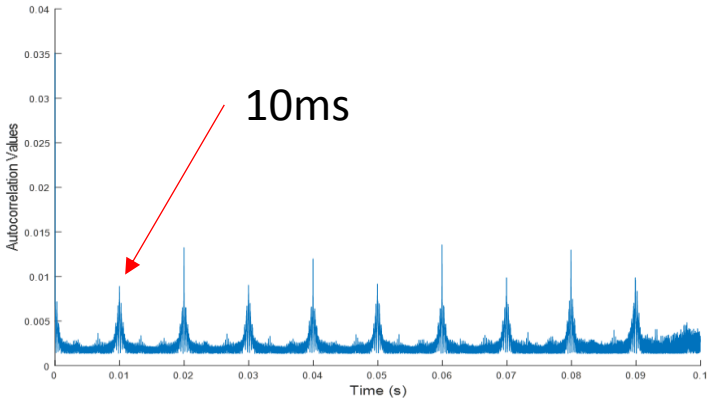

Figure 9 - Autocorrelation Results and highlighted repetition time of Indoor RFI for up to 100ms. This is plotted as this is the only recording with RFI with a repetition time longer than 1ms

The final parameters calculated from the binary mask of the RFI are presented in table 1.

Sample	Average RFI Pulse Length (µs)	RFI On Percentage	Average gap between RFI pulses (µs)
Lab – Surrey	1.29	25.56	3.75
Lab – Dstl	2.26	21.49	8.09
Indoors – Surrey	0.62	3.68	16.31
Outdoors - Surrey	0.24	3.38	7.12

Table 1 - RFI parameters calculated for the RFI samples

A Gaussian filtering technique was applied to the spectrum for the outdoor location (Figure 7d), with the Gaussian filter centred on the following frequencies: 1.57, 10.53 and 13.33 MHz. These

frequencies were chosen due to the significant peak at 1.57 and 13.33 MHz, whilst the 10.53 was a smaller peak to use as comparison.

The time-domain data produced by inverse Fourier transforming the filtered spectrum is plotted in Figure 10. The autocorrelation for 1.57 and 10.53 MHz is plotted in Figure 11.

A Gaussian filtering technique was applied to the spectrum for the outdoor location (Figure 7d), with the Gaussian filter centred on the following frequencies: 1.57, 10.53 and 13.33MHz. The time-domain inversed Fourier transformed data of the Gaussian filtered frequency-domain Fourier transformed data is plotted in Figure 10. the autocorrelation for 1.57 and 10.53 MHz is plotted in Figure 11.

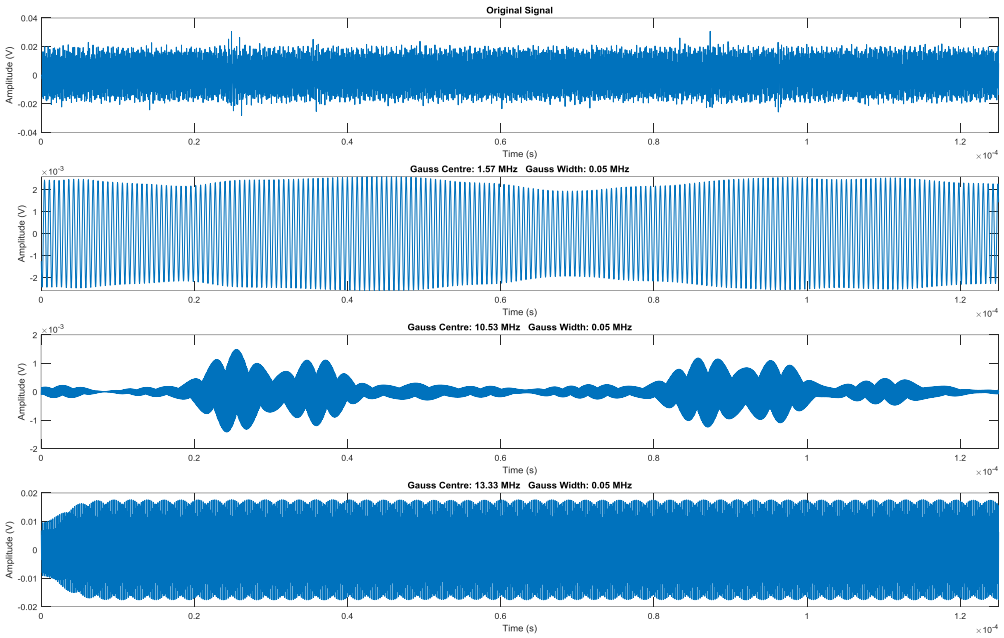

Figure 10 - Plots of the Inverse Fourier transformed data at the Gaussian filtered selected frequencies (1.57, 10.53 and 13.33 MHz), based on the FFT of the original outdoor sample in Figure 6

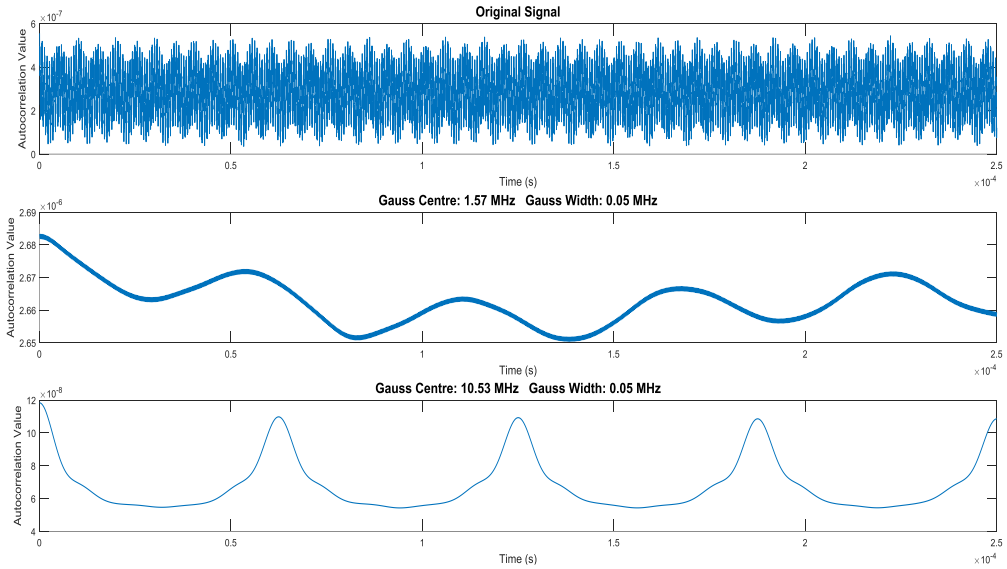

Figure 11 - Plots of the autocorrelation results for the Inverse Fourier transformed data at the Gaussian filtered selected frequencies (1.57 and 10.53 MHz) based on the FFT of the original outdoor sample signal in Figure 6

3.2 – Decision Tree Model

Three datasets were recorded to train and test the effectiveness of the decision tree model. The data sets were as follows:

- Data Set 1 (120 datasets = 51,200 units of data) - Identical NQR parameters with and without random pseudo-RFI that was used for training
- Data Set 2 (40 datasets = 24,576 units of data) - Varying NQR parameters to provide non-optimal NQR experimental data with and without pseudo-RFI
- Data Set 3 (200 datasets = 102,400 units of data) - Optimal NQR parameters with and without pseudo-RFI, to test the RFI suppression technique without any bias due to sub-optimal NQR parameters. This data was used in the validation trial.

Data collected in data series two and three were treated with the decision tree model to identify and remove (directly) the RFI.

The result of the Decision Tree identification and RFI direct removal method is presented in Figure 12. Figure 12a shows the demodulated and averaged signal for an experiment undertaken with eight echoes. The refocusing pulses are seen as white vertical bands that saturate the receiver. The rest of the signal is corrupted by RFI, making it unusable. Figure 12b shows the same data but treated with the RFI suppression method. The NQR signal is recovered and the sinusoidally-oscillating decaying-echoes are clearly seen.

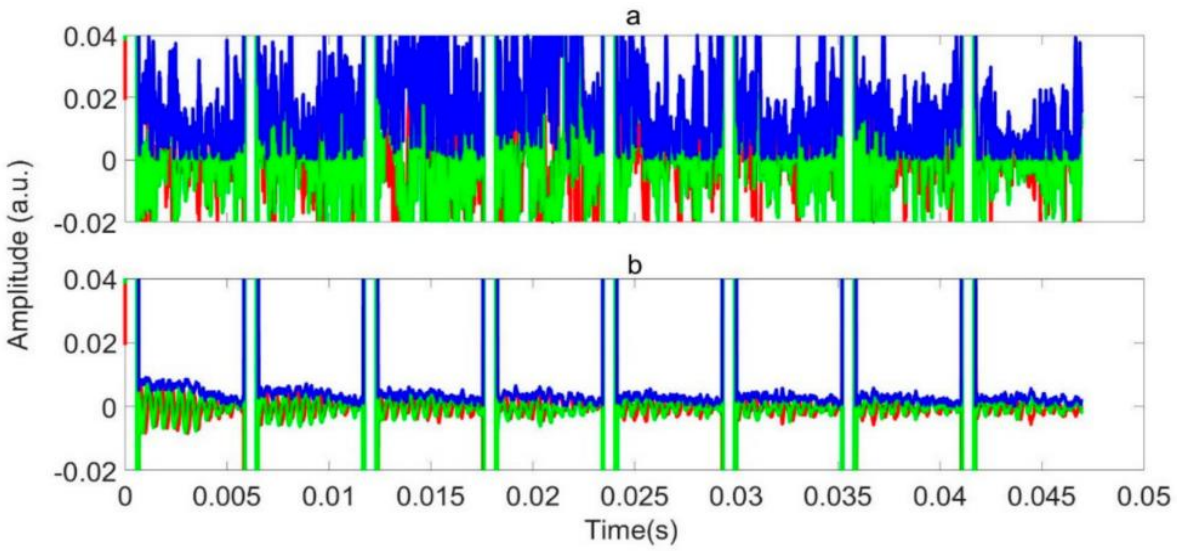

Figure 12 - An averaged and demodulated signal. The red, green, and blue lines represent the real, imaginary, and magnitude of the data, respectively: (a) without and (b) with the application of the RFI decision tree identification model

3.3 – Validation of the DT RFI identification and RFI Direct Removal

The results from the validation trial are presented in Figure 13, for the number of scans varying from 4 to 64. The aggregated results (over all scans) are presented in the overall ROC curve.

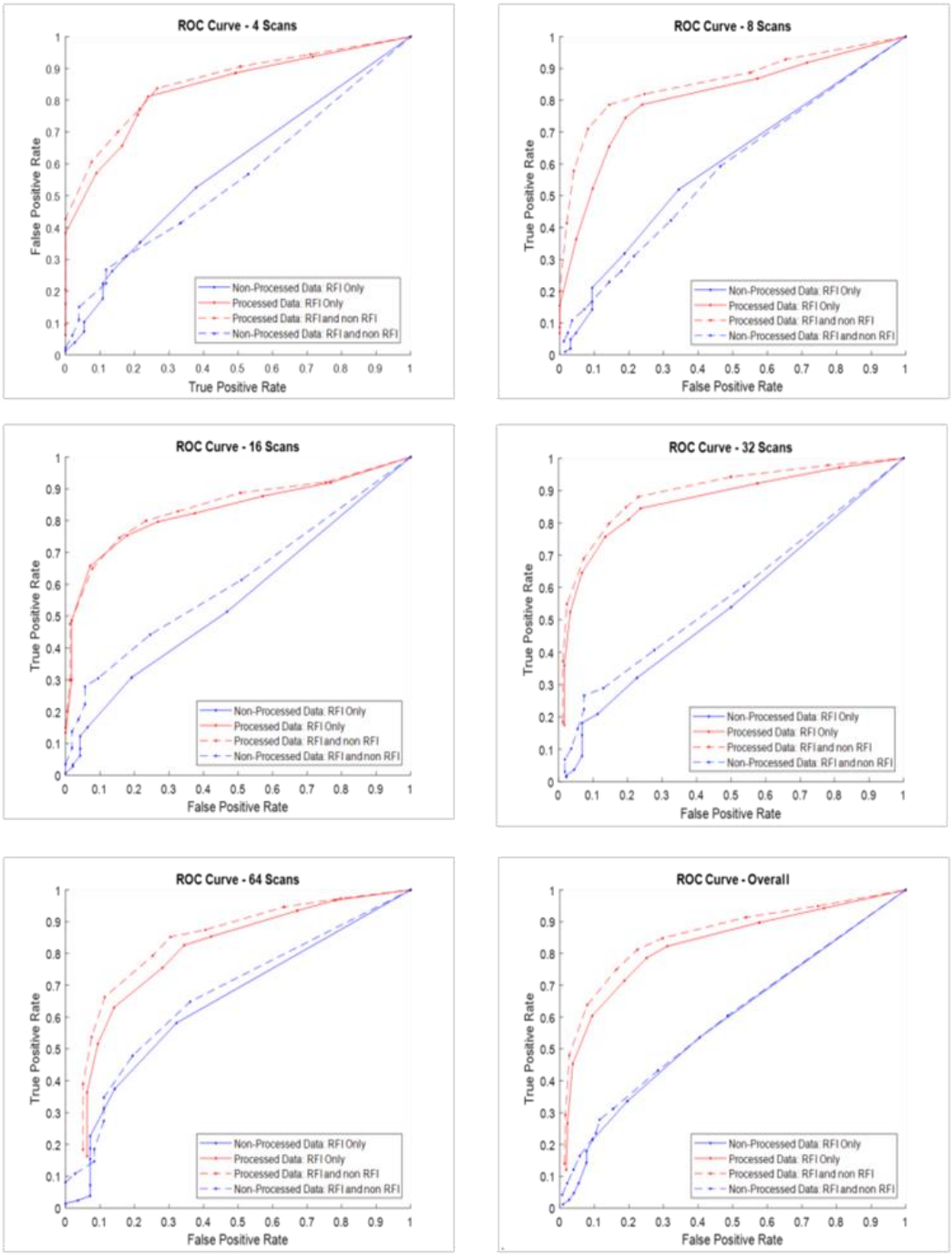

Figure 13 - ROC Plots for varying numbers of scans and overall (all of the ratings combined), which are processed by the DT RFI Identification and RFI direct removal algorithm (red curve) and not processed (blue curve), the solid lines represent results when all of the data contained RFI, dashed lines represent a mixture of RFI and non-RFI data

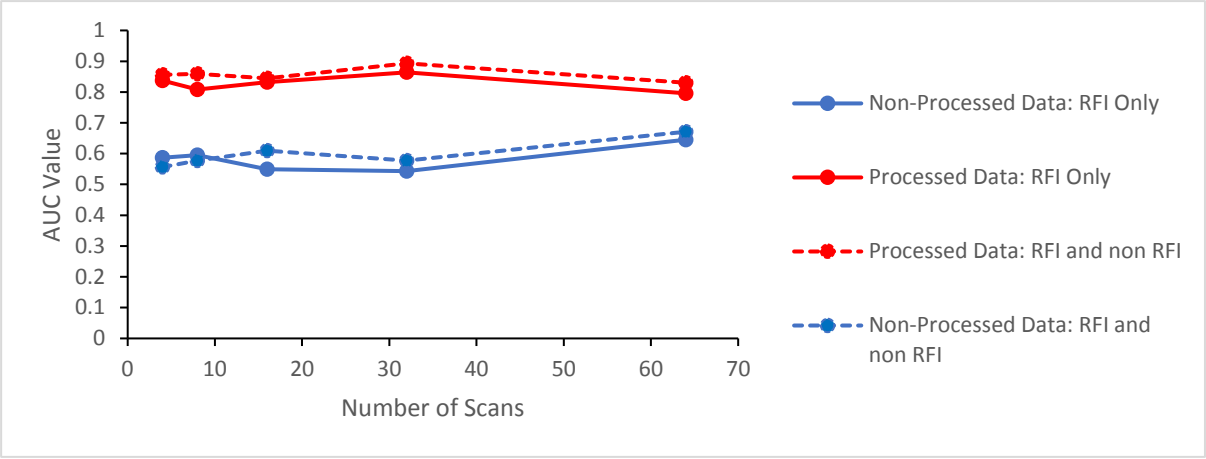

Figure 14 - AUC Values Vs. Number of Scans for the human validation

Figure 14 shows the AUC for the ROC curves in Figure 12, which shows a significant improvement in AUC values between processed data, which has values typically above 0.8, compared to 0.5 for non-processed data.

Figure 15 shows the average score provided by different volunteers for identical data across the different categories of data, and for different sample weights and number of scans. These values will show how different categories of data affected the average score provided by multiple volunteers, with processed data expected to be greater than non-processed data.

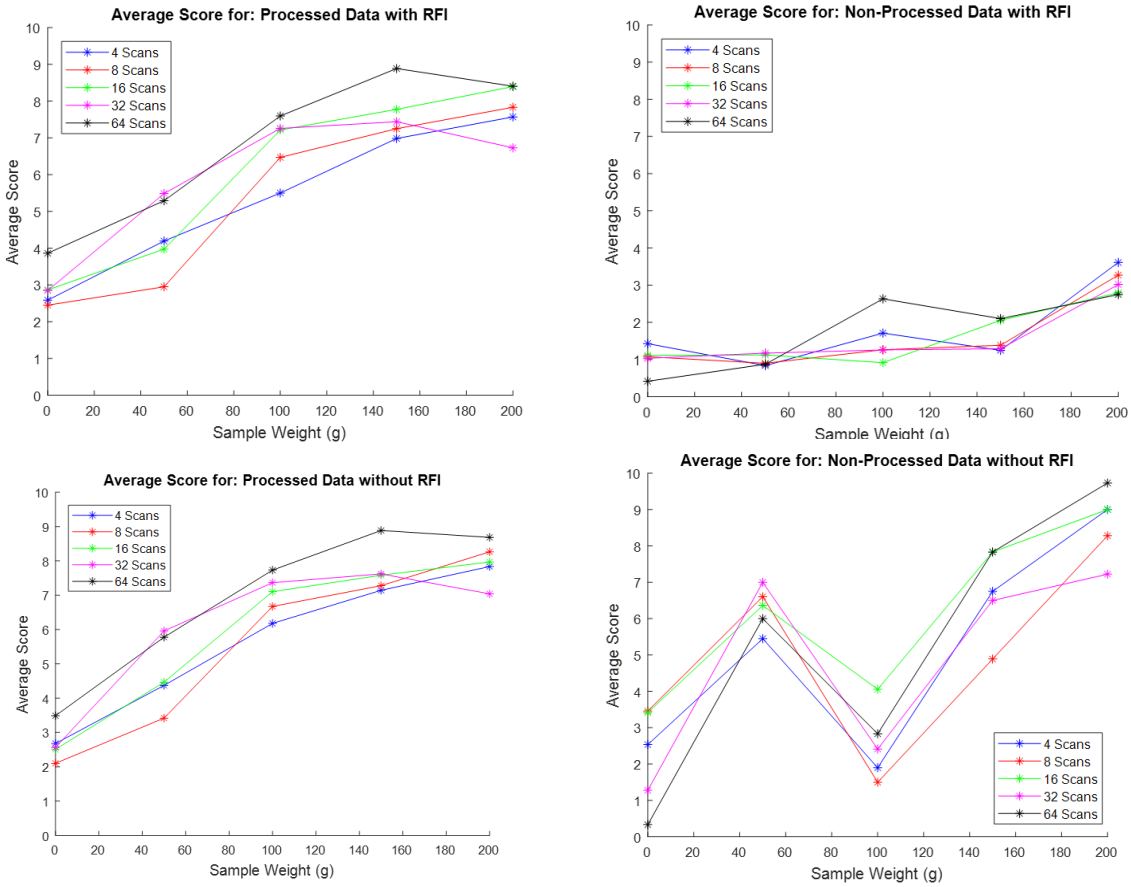

Figure 15 - Average Score for different categories of data, for datasets seen by multiple people, Top Left = Processed Data with RFI, Top Right = Non-Processed Data with RFI, Bottom Left = Processed Data without RFI, Bottom Right = Non-Processed Data without RFI

4 – Discussion

4.1 – RFI Characterisation

Analysis of the RFI characterisation data shows that any RFI suppression method will need to be able to cope with the large variety in RFI. For example, the spectra plotted in Figure 6, shows that the range of frequencies encountered can vary widely between locations, whilst 3 out of 4 recordings had the same frequency as the NQR frequency of sodium nitrite (3.6 MHz) used in the testbed. An effective suppression method, therefore, needs to cope with RFI at the same frequency as the NQR/NMR signal.

The variety of RFI is clearly visible in the plots shown in Figure 5, where there is repeating digital pulses of different lengths and repetition times. There are also repeating bursts of pulses with the same structure, as such in Figure 5(c), with the same three pulses repeating. In addition, the variability in the autocorrelation results, plotted in Figure 8 and Figure 9, show a wide range of repetition times ranging from micro to milliseconds. So, an NQR echo (e.g. 3ms) would record the same RFI multiple times within an NQR measurement.

Furthermore, the RFI parameters calculated for each location, (table 1), show that both laboratories have a higher percentage of signal that was digital RFI (25.5%) compared to the indoor location (3.7%). This means that in the laboratory, without shielding/suppression, each scan of an NQR measurement would have 25% of the NQR signal masked by RFI. In contrast with doing an NQR experiment at the indoor location, where each measurement would only have (3%) of the NQR signal per scan masked by RFI.

The difficulty of suppressing RFI is further increased by the variability within the same signal. For example, the Gaussian filtered inversed Fourier transformed results, in Figure 10, show that within the same sample, you can have digital RFI at some frequencies whilst encountering continuous RF at others. In this case, the different RFI have similar repetition times, as seen in the autocorrelation results (Figure 11). Dependable SNR improvements will, therefore, need a combination of RFI suppression techniques to cope with suppressing both digital RFI and continuous RFI.

4.2 – Decision Tree Model

There is a clear improvement moving from the non-processed to processed data (Figure 12), demonstrating the effectiveness of the RFI suppression technique. The non-processed data has no clear NQR signal, meaning the data is unusable, whereas the processed data clearly shows an NQR signal, which can be used to characterise the sample. In this case, the oscillations in the signal show the NQR frequency is 2 kHz off-resonance.

4.3 – Human Validation

The validation trial results demonstrate that the suppression method improves performance as summarised in the ROC curves and AUC values for processed data compared to non-processed data (Figure 13). These AUC values show that a high value of 0.89 was achieved using 32 scans, visible in Figure 14. Furthermore, the AUC value was not substantially lower for the lowest number of scans processed, meaning that it can achieve good results using minimal scans. This is exactly what is needed to allow this technique to be used for applications where time is short supply (e.g. scanning luggage at an airport).

Likewise, the average scores for each category of data, plotted in Figure 15, shows that processed data with RFI had higher ratings than the non-processed data, and the ratings increase with sample

weight and number of scans because the NQR echoes have a greater amplitude. The processed data that had no RFI was rated the same as processed with RFI, which means that processing data that didn't need processing doesn't reduce the average scores achieved. This means that this method does not reduce the NQR signal visibility of NQR data with no RFI. The non-processed data without RFI should have the same pattern of results as processed with RFI, but there is an anomaly with the 50g and 100g results, which are currently under investigation.

5 – Conclusion

This project created a new and novel machine learning based method to identify digital burst mode RFI and suppress it using a new method of RFI suppression known as 'direct removal'.

To better understand the variety of digital burst mode RFI that can be experienced, characterisation of RFI recorded in multiple locations was undertaken, and showed its varying complexity. These results showed that even laboratories have high levels of external RFI and require experiments to have Faraday shielding or RFI suppression techniques.

An experimental testbed was developed to undertake NQR experiments with controllable pseudo-RFI without external RFI. The data recorded from this was used to train the decision tree model and produce testing data.

A validation study was undertaken to produce the AUC values for varying number of scans. This was to determine the best AUC value of the technique that could be achieved but also to see how the number of scans affected the AUC values. The results showed that four scans produced the highest AUC per scan, meaning the suppression technique works effectively for time-sensitive applications (e.g. scanning luggage at an airport). However, a peak AUC value of 0.89 was achieved with 32 scans, perfect for non-time sensitive applications (e.g. research experiments).

6 – Future Work

The next step is to develop a new model that works on real RFI, which will involve recording new data with real RFI for training and testing. In addition, a series of blind trials will be conducted to determine how the AUC values of the model change as RFI changes over different time scales (days, weeks, months).

7 – Funding and Copyright

This research was funded by the U.K. Engineering and Physical Sciences Research Council (grant number EP/N018834/1). D.J.P. thanks the EPSRC Centre for Doctoral Training in Micro and NanoMaterials (University of Surrey) and the Defence Science and Technology Laboratory (Dstl), United Kingdom for financial support.

8 – References

1. *Applications of Low-Field NMR Techniques in the Characterisation of Oil Sand Mining, Extraction and Upgrading Processes.* **A. Kantzas, J. Bryan, A. Mai.** 1, 2005, The Canadian Journal of Chemical Engineering, Vol. 83, pp. 145-150.

2. *Determination of Total Fat and Moisture Content in Meat using Low Field NMR.* **Geir. Sorland, Per. Larsen, Frank. Lundby.** 2004, Meat Science, Vol. 66, pp. 543-550.

3. *A unilateral NMR magnet for sub-structure analysis in the built environment: The Surface GARField.* **P. McDonald, P. Aptaker, J. Mitchell et al.** 1, s.l. : Journal of Magnetic Resonance, 2007, Vol. 185.

4. *Joint TNT and RDX detection via quadrupole resonance.* **H. Xiong, J. Li, G. Barrall.** 4, s.l. : IEEE Transactions on Aerospace and Electronic Systems, 2007, Vol. 43.

5. **J. Michael, L. Buess, A. N. Garroway.** *Removing the effects of acoustic ringing and reducing temperature effects in the detection of explosives by NQR.* s.l. : United States Department of the Navy, 1992. US-5365171-A.

6. *Remote Sensing by Nuclear Quadrupole Resonance.* **A. Garroway, M. Buess, J. Miller.** 6, 2001, IEEE Transactions on Geoscience and Remote Sensing, Vol. 39, pp. 1108-1118.

7. *Signal Processing for NQR Discrimination of Buried Landmines.* **S. Tantum, L. Collins, L. Carin.** 1999, p. 9.

8. *Detecting NQR signals severely polluted by interference.* **W. Shao, J. Barras, K. Althoefer et al.** s.l. : Signal Processing, 2017, Vol. 138. 10.1016/j.sigpro.2017.03.032.

9. *Robust detection of nuclear quadrupole resonance signals in a non-shielded environment.* **T. Rudberg, A. Jakobsson.** Eusipco, s.l. : European Signal Processing Conference, 2011. 22195491.

10. **T. Brown, PJ. McDonald, R. Jenkinson.** *Active Elimination of Radio Frequency Interference for Improved Signal-To-Noise for In-Situ NMR/NQR Applications.* London : ESPRC, 2016.

11. *Decision tree pattern recognition model for radio frequency interference suppression in NQR experiments.* **M. Ibrahim, D. Parrish, T. Brown, P.J. McDonald.** 14, s.l. : Sensors (Switzerland), 2019, Vol. 19. 10.3390/s19143153.